HHS Public Access

Author manuscript

Anal Chem. Author manuscript; available in PMC 2016 April 21.

Published in final edited form as:

Anal Chem. 2015 April 21; 87(8): 4472–4478. doi:10.1021/acs.analchem.5b00421.

Automated Multiplexed ECL Immunoarrays for Cancer Biomarker Proteins

Karteek Kadimisetty[†], **Spundana Malla**[†], **Naimish Sardesai**[†], **Amit A. Joshi**[†], **Ronaldo C. Faria**[‖], **Norman Lee**[⊥], and **James F. Rusling**[†,‡,§,*]

[†]Department of Chemistry, University of Connecticut, Storrs, Connecticut 06269, United States [‡]Department of Cell Biology, University of Connecticut Health Center, Farmington, Connecticut 06032, United States [§]School of Chemistry, National University of Ireland at Galway, Galway, Ireland [‖]Departamento de Química, Universidade Federal de São Carlos, São Carlos, SP 13565-905, Brazil [⊥]Department of Pharmacology & Physiology, George Washington University, Washington, DC 20037, United States

Abstract

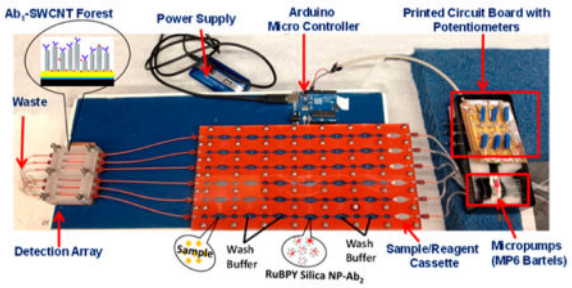

Point-of-care diagnostics based on multiplexed protein measurements face challenges of simple, automated, low-cost, and high-throughput operation with high sensitivity. Herein, we describe an automated, microprocessor-controlled microfluidic immunoarray for simultaneous multiplexed detection of small protein panels in complex samples. A microfluidic sample/reagent delivery cassette was coupled to a 30-microwell detection array to achieve sensitive detection of four prostate cancer biomarker proteins in serum. The proteins are prostate specific antigen (PSA), prostate specific membrane antigen (PSMA), platelet factor-4 (PF-4), and interlukin-6 (IL-6). The six channel system is driven by integrated micropumps controlled by an inexpensive programmable microprocessor. The reagent delivery cassette and detection array feature channels

*Corresponding Author: james.rusling@uconn.edu.

Notes

The authors declare no competing financial interest.

Supporting Information

Schematic of array; synthesis and characterization of RuBPY-Si nanoparticles; chemistry of ECL detection and detection array fabrication; sample/reagent cassette fabrication; micropumps and microprocessor control; microcontroller program; AFM of Ab_1 decorated immunoarray; Raman spectroscopy characterization of SWCNTs; array reproducibility; single biomarker detection; patient sample correlations and unspiked IL-6 results; and cleaning protocols. This material is available free of charge via the Internet at http://pubs.acs.org.

made by precision-cut 0.8 mm silicone gaskets. Single-wall carbon nanotube forests were grown in printed microwells on a pyrolytic graphite detection chip and decorated with capture antibodies. The detection chip is housed in a machined microfluidic chamber with a steel metal shim counter electrode and Ag/AgCl reference electrode for electrochemiluminescent (ECL) measurements. The preloaded sample/reagent cassette automatically delivers antigen proteins, wash buffers, and ECL RuBPY-silica–antibody detection nanoparticles sequentially. An onboard microcontroller controls micropumps and reagent flow to the detection chamber according to a preset program. Detection employs tripropylamine, a sacrificial reductant, while applying 0.95 V vs Ag/AgCl. Resulting ECL light was measured by a CCD camera. Ultralow detection limits of 10–100 fg mL^{-1} were achieved in simultaneous detection of the four protein in 36 min assays. Results for the four proteins in prostate cancer patient serum gave excellent correlation with those from single-protein ELISA.

Biomarker protein panels hold great promise for future personalized cancer diagnostics.[1–5] Widespread use of diagnostic protein measurements at clinical point-of-care will require simple, cheap, fast, sensitive, and automated assay devices.[4–6] Microfluidic devices integrated with sensitive nanomaterials-based measurement technologies have potential for future devices that fit these requirements.[7–11] Microfluidic immunoarrays have evolved to feature glass substrates with silicon patterns,[12] fabricated microchannels,[13] and valves[14] made with soft lithography. A major practical challenge involves integrating components into low-cost, fully automated devices for clinical use.[15]

Many current methods of specific biomarker protein detection are based on enzyme-linked immunosorbent assays (ELISA), including commercial magnetic bead-based devices.[10,16] Critical issues in these systems are cost, method complexity, and the need for technically trained operators and frequent maintenance. Immunoassays in general suffer from multiple operations to load samples and add reagents to block nonspecific binding, remove interferences, and detect target proteins. Significantly improved automation is needed to translate immunoassays to point-of-care use.[6,15] While semiautomated microfluidic reagent addition was reported previously for single- and two-antigen immunoassays, those systems do not achieve ultrasensitive detection and employ passive fluid delivery by a downstream syringe that requires operator attention.[17]

We previously developed modular microfluidic immunoarrays for multiplexed protein detection on 8-unit gold nanoparticle AuNP film sensor arrays using magnetic beads heavily loaded with enzyme labels and antibodies for detection.[18–20] In the latest version of this device, target proteins are captured online on the magnetic beads and delivered to an amperometric detection chamber. We have determined up to four biomarker proteins in serum at levels as low as 5 fg mL^{-1} with this system. We also developed microfluidic immunoarrays for electrochemiluminescence (ECL) detection[21] using a slightly different approach. Here, a thin pyrolytic graphite (PG) wafer was equipped with printed microwells, single-wall carbon nanotube (SWCNT) forests were grown in the microwells and decorated with antibodies, and $Ru(bpy)_3^{2+}$ (RuBPY) labels embedded in 100 nm silica nanoparticles coated with antibodies were used for protein detection at 10–100 fg mL^{-1} levels.[22] ECL detection obviates the need for individually addressable sensors, and the microwells need to

be separated in space on the chip only for light detection with a camera. While these systems afford some degree of automation, a skilled operator is needed to add samples and reagents and to coordinate assay timing.

In this article, we describe an inexpensive automated multiplexed protein immunoarray featuring an onboard microprocessor to control micropumps[23] and a microfluidic sample/reagent cassette upstream of a microwell ECL immunoarray (Figure 1 and Supporting Information Scheme S1). The microfluidic channels are precision cut from silicone gaskets. The system automatically delivers all necessary samples and reagents and controls timing of sample–sensor and detection particle incubations. The detection module features six 60 μL microfluidic channels on a single PG chip with 30 computer-printed microwells containing dense, upright SWCNT forests decorated with capture antibodies. We demonstrate the properties of the device by simultaneous detection of four proteins employing 120 nm RuBPY-silica (RuBPY-Si) nanoparticles coated with secondary antibodies (Ab_2), with detection by CCD camera. We targeted a general panel of prostate cancer biomarkers including prostate specific antigen (PSA),[24,25] interleukin-6 (IL-6), platelet factor-4 (PF-4), and prostate specific membrane antigen (PSMA).[26] Simultaneous detection of the four proteins in undiluted calf serum was achieved with high specificity and selectivity in 36 min assays, with detection limits of 10–100 fg mL^{-1}. Assays on human serum samples from prostate cancer patients confirmed very good correlations with single-protein ELISAs.

EXPERIMENTAL SECTION

Chemicals

Full experimental details are in the Supporting Information. Pooled human serum was from Capital Biosciences, and individual patient serum samples were provided by George Washington University Hospital. RuBPY-Si nanoparticles with average diameter 121 ± 9 nm (Figure S1) were prepared and coated with layers of polydiallyldimethylammonium chloride (PDDA) and poly(acrylic acid) (PAA) and were then covalently linked to secondary antibodies (Ab_2) as described previously.[27] Two RuBPY-Si detection nanoparticles were made, one with antibodies for PSA (PSA-Ab_2) and IL-6 (IL-6-Ab_2) and a second featuring PSMA-Ab_2 and PF-4-Ab_2. We measured averages of 4.6×10^5 RuBPY and 44 Ab_2 per Si nanoparticle (Figure S2). Immunoreagents were dissolved in pH 7.2 phosphate buffered saline (PBS). Co-reactant solution to develop ECL was 200 mM tripropylamine (TPrA) with 0.05% Tween-20 (T_{20}) and 0.05% Triton-X in 0.2 M phosphate buffer. Calf serum, as a surrogate for human serum, was used to dissolve standard proteins.[28]

Microfluidic Device

Figure 1 shows the automated microfluidic immunoarray featuring (i) printed-circuit board (PCB)-linked, microprocessor-controlled micropumps, (ii) six-channel sample/reagent delivery cassette, and (iii) six-channel microfluidic detection array. A PCB circuit design was constructed to serve six micropumps. Micropumps (Mp6, Bartels) featuring piezo-actuated membranes were optimized to 155 ± 1.5 μL min^{-1} by tuning potentiometers for each pump (Figure S3). An Arduino microcontroller was used to switch on and off

micropumps according to a preset program to deliver sample and immunoreagents and to stop flow for incubations (Figure S4).

Microfluidic channels were made by precision cutting 0.80 mm silicone gaskets (MSC industrial Supply) with the desired patterns using an inexpensive, programmable Accugraphic Klic-N-Kut (KNK) groove cutting machine. The cut gaskets (Figure 2A) were placed between two machined hard PMMA plates (Figure 2B, C) to assemble the final sample/reagent delivery cassette (Figure 2D. The final assembled sample/reagent delivery cassette was 11 in. × 5.5 in. with six channels, each having seven loading chambers separated individually by smaller air-filled channels to ensure delivery of reagents without mixing (Figure 2D). The top PMMA plate was machined with 1 mm diameter holes to fill the chambers, and the bottom plate has screw holes to tighten and seal the assembly. Each chamber holds 80 μL volume. Chambers were prefilled by syringe, and openings were sealed with tape

The detection chamber also features six microfluidic channels (60 ± 2 μL) cut from a silicone gasket that is then placed on a thin 2 × 3 $in.^2$ PG wafer with computer-printed microwells[22,29] (Figure 2E). This gasket (Figure 2F) is placed on the PG slab and sealed by bolting it between two flat machined PMMA plates. The top PMMA plate (Figure 2G) houses symmetrically placed Ag/AgCl reference and stainless steel metal shim (MSC Industrial Supply) counter electrodes that are aligned into each of the six channels, completing a symmetric electrochemical cell with the entire PG chip as the working electrode (Figure 2H). The top PMMA plate is fitted with optically clear acrylic[22] windows above each microwell channel to pass ECL light to a CCD camera.

Dense SWCNT forests were grown in each microwell (volume 2 ± 0.5 μL).[22,30] Tapping-mode atomic force microscopy and Raman spectrum confirmed vertical-aligned SWCNT forests in the microwells with a surface roughness of 17 ± 4 nm surrounded by the hydrophobic printed wall (Figures S5 and S6). Terminal carboxylic groups on SWCNTs were activated by freshly prepared 400 mM EDC + 100 mM NHSS to attach cognate primary antibodies (Ab_1) by amidization.[22,28]

Immunoassay Protocol

The Ab_1-decorated PG chip microwells containing SWCNT-Ab_1 were spotted with 2% BSA in PBS containing 0.05% Tween 20 (T20) to minimize nonspecific binding (NSB). The PG chip was assembled into the detection chamber, which was then connected to a prefilled sample/reagent cassette. The Arduino microcontroller precisely times sample and reagent delivery by micropumps to the detection chamber according to a preoptimized program.

The immunoassay protocol was developed by optimizing micropump flow rates (Figure 3), using a 15 turn 10 kOhm. Flow rates were optimized at 155 μL^{-1} by carefully changing the amplitude of all of the micropumps while turning the screw of the potentiometer. Incubation times were also optimized for protein binding steps to ensure high sensitivity and reproducibility with spot-to-spot variability < 10%. The capture antibody-decorated immunoarray sensor chamber was incubated with 2% BSA in PBS T20 prior to the assay to

block NSB for 50 min and was then washed with PBS T20 and PBS. Patient serum samples of 5–10 μL were diluting 30–500-fold in calf serum prior to performing the assay.

Once the sample/reagent cassette is loaded, the micropumps turn on initially for 55 s to deliver sample to the detector. Second, flow is stopped for 20 min to allow analyte proteins in the sample to bind Ab_1 in the microwells. Next, micropumps activate again for 220 s to deliver wash buffer to move the sample solution and unbound target proteins out of the detection channels. Then, pumps deliver RuBPY-Si–Ab_2 nanoparticles to the detector, and a 900 s stopped-flow incubation follows. Flow then turns on to wash away unbound RuBPY-silica nanoparticles. Finally, with the detection chamber in a dark box, micropumps deliver TPrA co-reactant to the detection channels (see Scheme S2), and a potential of 0.95 V vs Ag/AgCl is applied for 400 s to generate ECL from RuBPY-Si particles while a CCD camera captures the ECL light.

RESULTS

Reproducibility

Relative ECL intensities for the immunoarray with controls (undiluted calf serum) showed spot-to-spot variability < 9% for $n = 5$ per channel (Figure S7). The first and last channels were used for controls, and the inner four channels were used for detection of the four target proteins. Array-to-array reproducibility of background signals was measured by injecting undiluted calf serum into all six channels (Figure S7), giving array-to-array variability ~ 11%. Calibrations were then done for each of the four individual proteins in calf serum, giving relative standard deviations < 10% (see Figures S8 and S9).

Multiplexed Detection

Calibration studies were done by dissolving the four target protein standards in calf serum, which serves as a human serum surrogate without human proteins.[30] Thus, the four proteins were detected selectively and simultaneously from samples containing thousands of proteins. Channels 1 and 6 in the detection array were used as controls, and only undiluted calf serum was introduced into these channels. Channels 2–5 were assigned for detection of IL-6, PF4, PSMA, and PSA, respectively. Simultaneous detection was achieved by using a mixture of the 2 RuBPY-Si–Ab_2 detection nanoparticles that were each decorated with antibodies for two of the four proteins. RuBPY-Si-Ab_2 were prepared with 4.5×10^5 [[Ru-$(bpy)_3]^{2+}$] ions and 44 Ab_2 per particle (see Supporting Information).

CCD camera images of the ECL response for multiple protien detection (Figure 4) illustrate increased ECL light with increased concentrations of proteins in the mixture. Using the average ECL signal divided by the average blank on each chip, we achieved dynamic ranges for of 100 fg mL^{-1} to 1 ng mL^{-1} for PSA, 100 fg mL^{-1} to 10 ng mL^{-1} for PSMA, and 100 fg mL^{-1} to 5 ng mL^{-1} for IL-6 and PF-4 (Figure 5). There is a small amount of nonlinearity in these curves, so power series curve fits were used to give correlation coefficients (R) ≥ 0.99. These curves are well-suited for use in target protein determinations. Limits of detection (LD) were measured (3 standard deviations of the zero protein control signal) at 50 fg mL^{-1} for PSA, 100 fg mL^{-1} for PSMA and IL-6, and 10 fg mL^{-1} for PF4.

Assay Validation

Nine serum samples from prostate cancer patients and two samples from cancer-free patients were analyzed and compared with results from single-protein ELISA. ELISA was done on the samples using commercially available kits: PSA (RAB0331 human PSA total ELISA kit), IL-6 (RAB0306 human IL-6 total ELISA kit), and PF-4 (RAB0402 human PF-4 total ELISA kit) were obtained from Sigma-Aldrich. PSMA (EL008782HU-96 human PSMA/FOLH1 ELISA kit) was obtained from Lifeome Biolabs/Cusabio. Samples were diluted 30–500-fold in calf serum prior to performing the assay to bring the ECL responses into an acceptable range based on the calibration curves. Concentrations of PF-4, PSMA, and PSA fall within the detection limits of their respective ELISAs, but IL-6 concentrations in the serum samples were well below the detection limit of its ELISA. For the validation study, we spiked the samples with known concentrations of IL-6, from 100 to 500 pg mL^{-1}, and then analyzed them by both methods. The immunoarray values corresponded well with the ELISA values (Figure 6). Variance in replicate assays resulted in small variations in averages of the spiked IL-6 human serum results for both ECL and ELISA, suggesting that 50 pg mL^{-1} differences are difficult to distinguish in the 100–500 pg mL^{-1} range, but a 100 pg mL^{-1} difference is easily distinguished by the immunoarray. This does not present a diagnostic problem since the threshold between noncancer and cancer patients is in the 15–20 pg mL^{-1} range.[26] Unspiked patient samples gave IL-6 values from <1 to ~17 pg mL^{-1} (Figure S10)

Linear correlation plots of the ELISA vs immunoarray data (Figure 7 and Table S1) gave slopes that were all close to 1.0: 1.14 ± 0.1 for IL-6, 0.97 ± 0.046 for PF-4, 1.11 ± 0.035 for PSA, and 0.96 ± 0.029 for PSMA. Intercepts of these plots were within 1 standard deviation of zero: 0.022 ± 0.029 for IL-6, 0.011 ± 0.029 for PF-4, −0.0367 ± 0.158 for PSA, and −0.013 ± 0.021 for PSMA. The excellent correlation of the automated immunoassay results with those from ELISAs on patient serum samples confirms the high selectivity and specificity of the assay for each of the four proteins in the presence of thousands of other proteins in human serum, many at much higher concentrations than the target analytes.[31]

DISCUSSION

These results demonstrate the use of an automated immunoarray requiring minimal operator attention for sensitive, simultaneous quantitative measurements of up to four proteins. Once the sample/reagent cassette is filled, automated operation and detection take less than 40 min. Including two control lanes in the detector enables the average protein signals to be divided by the average blank signal for each individual assay to minimize chip-to-chip variability (Figure S9). Ultrasensitive detection in serum was achieved down to concentrations of 10 fg mL^{-1} over dynamic ranges of 5 orders of magnitude in concentration (Figure 5). We found relative standard deviations ranging from ±1 to 7% for all proteins except IL-6, where RSD ranged up to ±15% at 1 pg mL^{-1} and below. These standard deviations are acceptable for accurate assays, as shown by the good agreement of patient sample results with ELISA, and were comparable or better than standard deviations from ELISA (Figure 6).

Immunoarray assays showed very good correlations with standard ELISA for serum from prostate cancer patients using only 5–10 μL of sample (Figures 6 and 7). Selectivity and specificity of the assay were confirmed by accurate determination of the four analyte proteins in human serum, which contains thousands of potentially interfering proteins.[31] In addition, the immunoarray successfully determined levels of IL-6 below 3 pg mL^{-1} (Figure S10), which is below the detection limit of ELISA.

Automation of the methodology is under the control of an Arduino microcontroller that turns the micropumps on and off according to a preset program and controls the flow of reagents from the preloaded sample/reagent cassette to the detection chamber and then to waste (Figure 1). This open-source electronic platform is very cheap and utilizes free software. The program is easily changed to accommodate changes in the assay protocol, so the system can be adapted to any reasonable set of assay conditions.

The microfluidic channels (Figure 2) in the sample/reagent cassette and the detection chamber were precision cut using an inexpensive, programmable KNK cutter from a 0.8 mm silicon gasket of the kind used in automobile engines. The cut gaskets are then press-fitted between appropriately machined hard plastic plates to seal the channels and provide inlets and outlets. This approach is cheap and versatile, allows rapid design changes, and avoids lithography, molding, and polymerization steps. The resulting system performs as well as or better than a nonautomated ECL microfluidic immunoarray that we constructed using molded, polymerized polydimethylsiloxane (PDMS) channels.[22] The sample/reagent cassette and detection device used here cost $15; micropumps and other electronics cost a total of $450. All of these components are fully reusable, making the assays very economical.

We have adapted several features from our earlier non-automated immunoarrays to the automated system. Utilization of the SWCNT forests in detector chip microwells provides a high-area nanostructured surface to enhance antibody concentration in each microwell, contributing significantly to the immunoarray's high sensitivity.[27,28] The multilabel RuBPY-Si-Ab_2 nanoparticle provides nearly 1/2 million RuBPY labels per bound target protein, providing the second important component, ultrasensitive detection. The use of TPrA in the Triton X-100 detergent solution as co-reactant allows a detection potential of 0.95 V vs Ag/AgCl to be achieved, where only TPrA is oxidized electrochemically to enhance production and deprotonation of $TPrA^{*+}$ to drive the complex redox process that provides electronically excited $[RuBPY]^{2+*}$ for ECL.[22,27,32]

In summary, a cheap, automated, and microprocessor controlled microfluidic immunoarray has been developed for simultaneous detection of four prostate cancer biomarkers at high sensitivity. Inexpensive components and simple fabrication procedures facilitate the production of a low-cost device costing about $550 in materials. The device is versatile and, in principle, can be reprogrammed for the detection of virtually any small protein panel.

Supplementary Material

Refer to Web version on PubMed Central for supplementary material.

Acknowledgments

This work was supported financially by grant nos. EB016707 and EB014586 from the National Institute of Biomedical Imaging and Bioengineering (NIBIB), NIH. The authors thank Daniel Daleb for assistance with device design and fabrication.

References

1. Hawkridge AM, Muddiman DC. Annu Rev Anal Chem. 2009; 2:265–277.
2. Wulfkuhle JD, Liotta LA, Petricoin EF. Nat Rev Cancer. 2003; 3:267–275. [PubMed: 12671665]
3. Kingsmore SF. Nat Rev Drug Discovery. 2006; 5:310–320.
4. Giljohann DA, Mirkin CA. Nature. 2009; 462:461–464. [PubMed: 19940916]
5. Rusling JF, Kumar CV, Gutkind JS, Patel V. Analyst. 2010; 135:2496–2511. [PubMed: 20614087]
6. Rusling JF. Anal Chem. 2013; 85:5304–5310. [PubMed: 23635325]
7. Janasek D, Franzke J, Manz A. Nature. 2006; 442:374–380. [PubMed: 16871204]
8. Zhang C, Xing D. Chem Rev. 2010; 110:4910–4947. [PubMed: 20394378]
9. Whitesides GM. Nature. 2006; 442:368–373. [PubMed: 16871203]
10. Wang J. Biosens Bioelectron. 2006; 21:1887–1892. [PubMed: 16330202]
11. Rusling JF, Bishop GW, Doan NM, Papadimitrakopoulos F. J Mater Chem B. 2014; 2:12–30.
12. Gervais L, de Rooij N, Delamarche E. Adv Mater. 2011; 23:151–176.
13. Hulme SE, Shevkoplyas SS, Whitesides GM. Lab Chip. 2009; 9:79–86. [PubMed: 19209338]
14. Weibel DB, Kruithof M, Potenta S, Sia SK, Lee A, Whitesides GM. Anal Chem. 2005; 77:4726–4733. [PubMed: 16053282]
15. Chin CD, Linder V, Sia SK. Lab Chip. 2012; 12:2118–2134. [PubMed: 22344520]
16. Beveridge JS, Stephens JR, Williams ME. Annu Rev Anal Chem. 2011; 4:251–273.
17. (a) Linder V, Sia SK, Whitesides GM. Anal Chem. 2005; 77:64–71. [PubMed: 15623279] (b) Chin CD, Laksanasopin T, Cheung YK, et al. Nat Med. 2011; 17:1015–1020. [PubMed: 21804541]
18. Chikkaveeraiah BV, Mani V, Patel V, Gutkind JS, Rusling JF. Biosens Bioelectron. 2011; 26:4477–4483. [PubMed: 21632234]
19. Malhotra R, Patel V, Chikkaveeraiah BV, Munge BS, Cheong SC, Zain RB, Abraham MT, Dey DK, Gutkind JS, Rusling JF. Anal Chem. 2012; 84:6249–6255. [PubMed: 22697359]
20. Otieno BA, Krause CE, Latus A, Chikkaveeraiah BV, Faria RC, Rusling JF. Biosens Bioelectron. 2014; 53:268–274. [PubMed: 24144557]
21. Forster RJ, Bertoncello P, Keyes TE. Annu Rev Anal Chem. 2009; 2:359–385.
22. Sardesai NP, Kadimisetty K, Faria RC, Rusling JF. Anal Bioanal Chem. 2013; 405:3831–3838. [PubMed: 23307128]
23. Arduino. http://arduino.cc
24. Telesca D, Etzioni R, Gulati R. Biometrics. 2008; 64:10–19. [PubMed: 17501937]
25. Lilja H, Ulmert D, Vickers AJ. Nat Rev Cancer. 2008; 8:268–278. [PubMed: 18337732]
26. Chikkaveeraih BV, Bhirde A, Malhotra R, Patel V, Gutkind JS, Rusling JF. Anal Chem. 2009; 81:9129–9134. [PubMed: 19775154]
27. Sardesai N, Pan S, Rusling JF. Chem Commun. 2009:4968–4970.
28. Malhotra R, Papadimitrakopoulos F, Rusling JF. Langmuir. 2010; 26:15050–15056. [PubMed: 20731335]
29. Tang CK, Vaze A, Rusling JF. Lab Chip. 2012; 12:281–286. [PubMed: 22116194]
30. Yu X, Munge B, Patel V, Jensen G, Bhirde A, Gong JD, Kim SN, Gillespie J, Gutkind JS, Papadimitrakopoulos F, Rusling JF. J Am Chem Soc. 2006; 128:11199–11205. [PubMed: 16925438]
31. Pieper R, Gatlin CL, Makusky AJ, Russo PS, Schatz CR, Miller SS, Su Q, McGrath AM, Estock MA, Parmar PP, Zhao M, Huang S, Zhou J, Wang F, Esquer-Blasco R, Anderson NL, Taylor J, Steiner S. Proteomics. 2003; 3:1345–1364. [PubMed: 12872236]

32. Miao W, Bard AJ. Anal Chem. 2004; 76:5379–5386. [PubMed: 15362895]

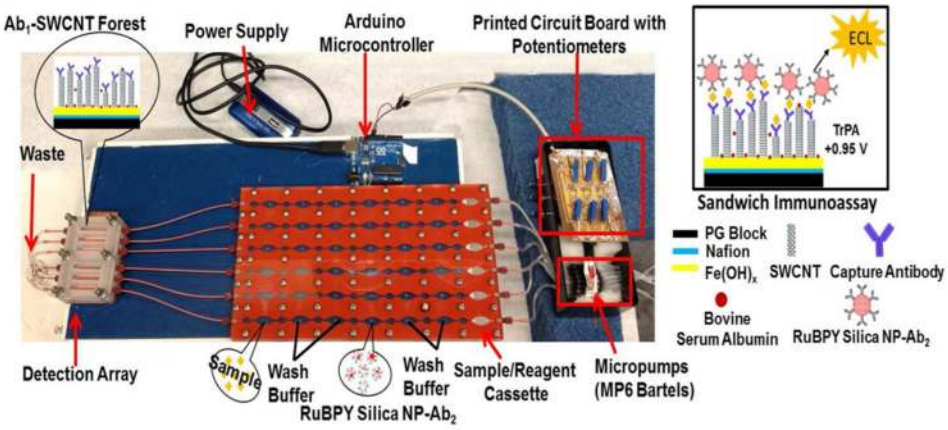

Figure 1.

Automated microfluidic system featuring a 30-microwell detection array connected to sample/reagent cassette and PCB-controlled micropumps. An onboard-programmed Arduino microcontroller runs a micropump program to achieve the assay.

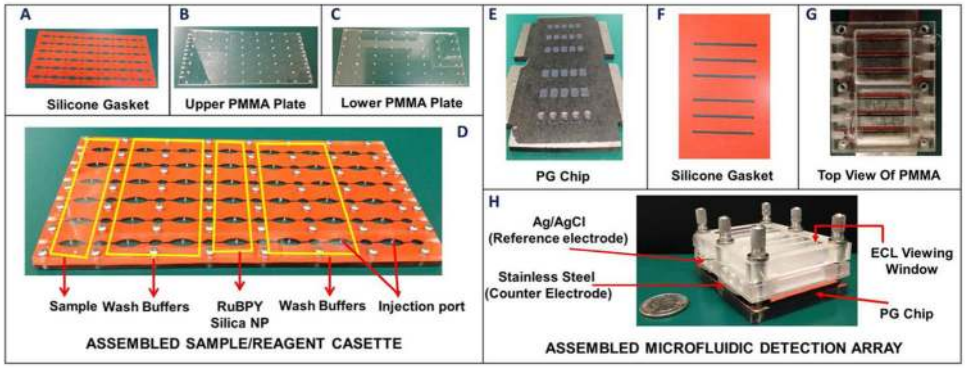

Figure 2.

Immunoarray components. Left panels shows the sample/reagent delivery cassette consisting of (A) a 0.8 mm silicon gasket cut to scale using a KNK cutter, (B) an upper hard PMMA plate machined with injection ports, (C) a lower PMMA plate, and (D) the assembled sample/reagent cassette shown with chambers for solutions, assembled with screws. Right panels show the detection array consisting of (E) a PG wafer with computer-printed microwells, (F) a silicone gasket cut with six precision channels, (G) the top PMMA plate showing an attached stainless steel counter electrode on top with clear windows for ECL detection and Ag/AgCl reference electrode, and (H) the fully assembled microfluidic detection array with clear windows in the top PMMA plate positioned above the microwells in each channel.

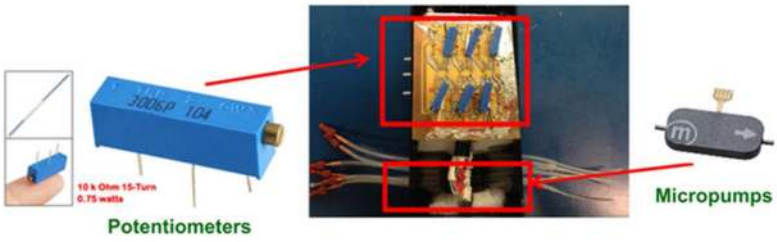

Pump #	Pump 1	Pump 2	Pump 3	Pump 4	Pump 5	Pump 6
Average Flow Rate, μL min^{-1}	155.0	152.2	155.4	156.2	154.4	156.2
STDEV (5 trials)	0.71	1.48	2.51	2.86	2.30	2.49
Average Flow Rate = 154.9 μL min^{-1}						
Standard Deviation in Flow Rates Between Pumps = ± 1.5 μL min^{-1}						
Relative Standard Deviation in Flow Rates Between Pumps = 1 %						

Figure 3.

Optimization of flow rates using 10 kOhm potentiometers (one for each micropump) to set the amplitude of each micropump. Table shows average flow rate of all micropumps along with individual flow rates and standard deviations.

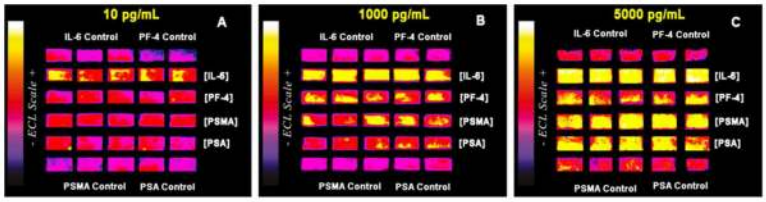

Figure 4.

Recolorized CCD images of three microfluidic immunoarray experiments showing reproducibility in simultaneous detection of IL-6, PF-4, PSMA, and PSA in calf serum with respective controls at protein concentrations of (A) 10 pg mL^{-1}, (B) 1000 pg mL^{-1}, and (C) 5000 pg mL^{-1}.

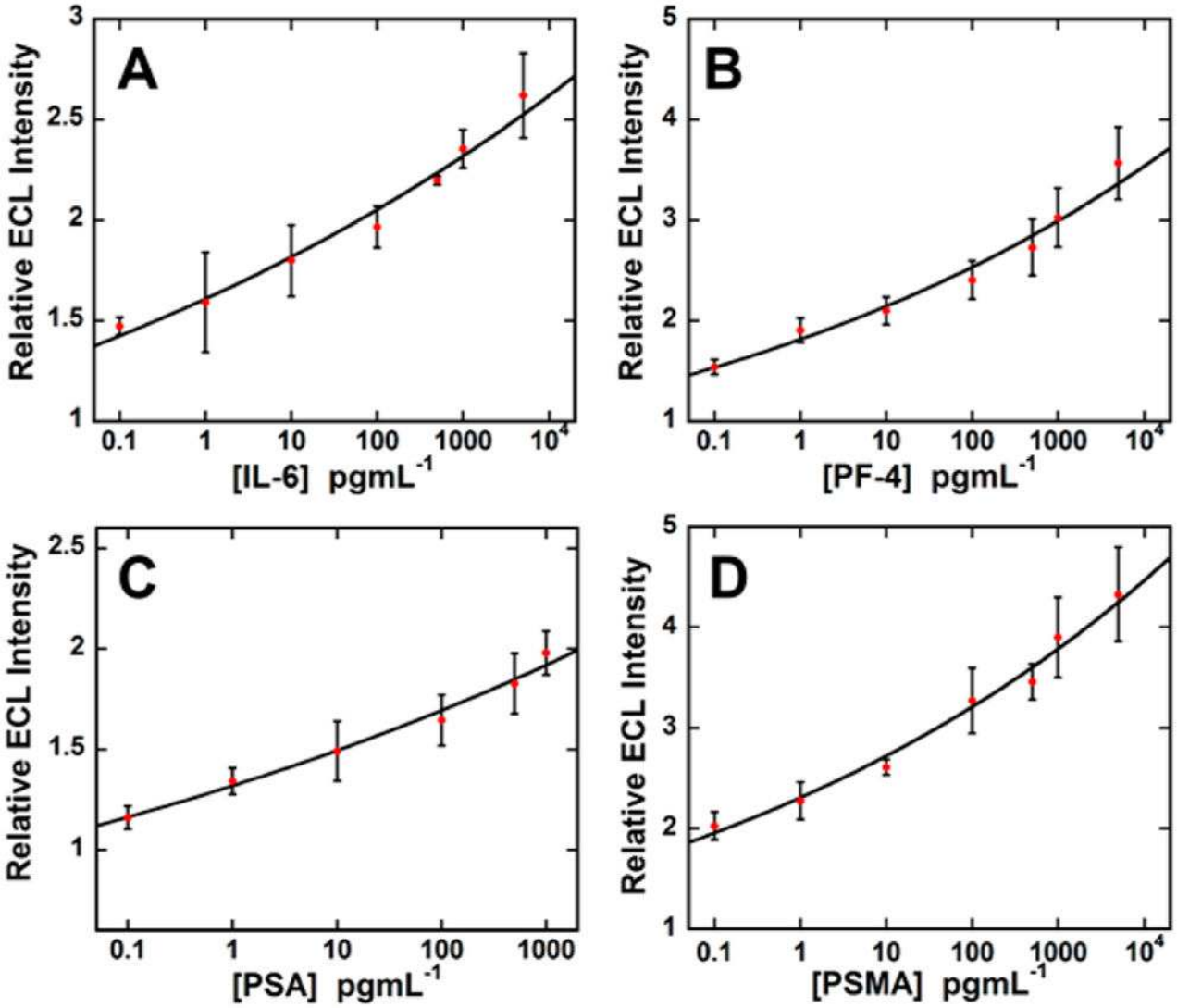

Figure 5.

Calibration curves in undiluted calf serum, with ECL responses integrated over 400 s, for (A) IL-6, (B) PF-4 concentration on ECL signal, (C) influence of PSA concentration on ECL signal, and (D) influence of PSMA concentration on ECL signal. Error bars show standard deviation; $n = 5$.

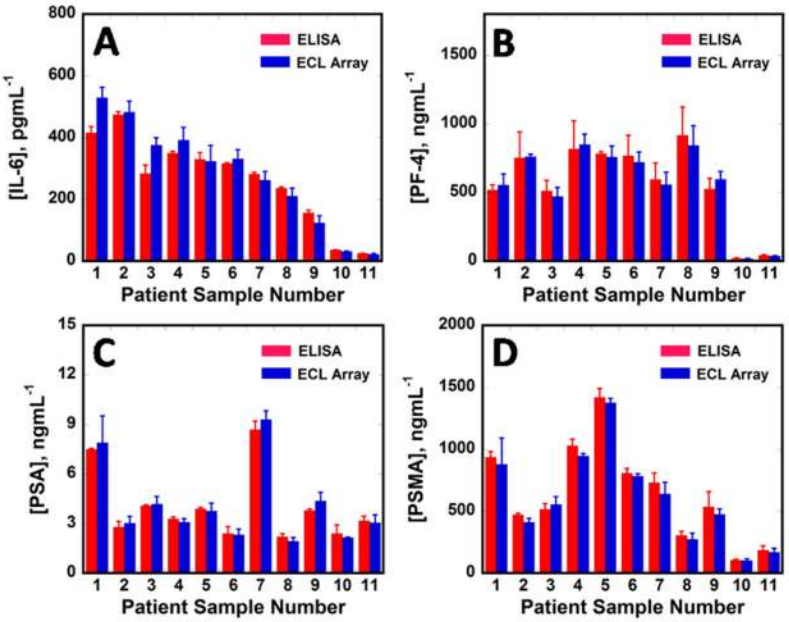

Figure 6.

Assays of human serum samples comparing immunoarray results to those of single-protein ELISAs. Samples 1–9 are from prostate cancer patients and 10 and 11 are from cancer-free patients. (A) IL-6 was spiked into samples as follows: 1 (500 pg mL^{-1}), 2 (450 pg mL^{-1}), 3 (400 pg mL^{-1}), 4 (350 pg mL^{-1}), 5 (300 pg mL^{-1}), 6 (250 pg mL^{-1}), 7 (200 pg mL^{-1}), 8 (150 pg mL^{-1}), 9 (100 pg mL^{-1}), 10 (30 pg mL^{-1}), and 11 (20 pg mL^{-1}). (B) PF-4, (C) PSA, and (D) PSMA. Error bars are standard deviations for ECL (n = 5) and ELISA (n = 3).

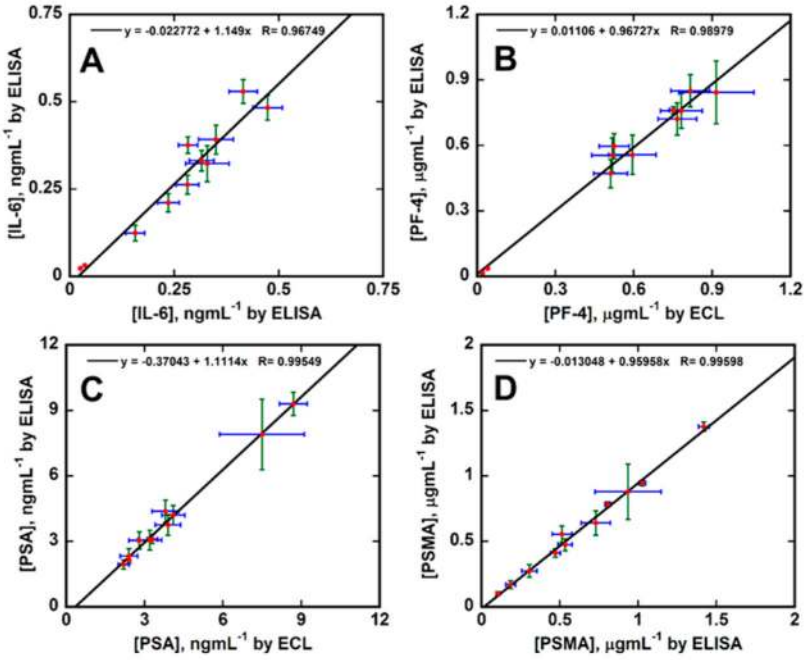

Figure 7.

Correlation plots of ELISA vs ECL immunoarray for human serum samples for (A) IL-6, (B) PF-4, (C) PSA, and (D) PSMA.